SCIENTIFIC REPORTS

OPEN

SUBJECT AREAS:
BIOGEOCHEMISTRY
GEOCHEMISTRY

Received
18 September 2014

Accepted
4 December 2014

Published
13 January 2015

Correspondence and requests for materials should be addressed to F.I.V. (floor.vandevenne@uantwerpen.be)

Landscape cultivation alters $\delta^{30}Si$ signature in terrestrial ecosystems

Floor I. Vandevenne[1], Claire Delvaux[2], Harold J. Hughes[2], Luc André[2], Benedicta Ronchi[3], Wim Clymans[4], Lúcia Barão[1], Jean-Thomas Cornelis[5,6], Gerard Govers[3], Patrick Meire[1] & Eric Struyf[1]

[1]Department of Biology, Research Group Ecosystem Management, University of Antwerp, Wilrijk, Belgium, [2]Department of Geology and Mineralogy, Royal Museum for Central Africa, Tervuren, Belgium, [3]Department of Earth and Environmental Sciences, Catholic University of Leuven, Heverlee, Belgium, [4]Department of Geology, Lund University, Lund, Sweden, [5]Department BIOSystem Engineering, University of Liège, Gembloux, Belgium, [6]Earth and Life Institute, Université catholique de Louvain, Louvain-la-Neuve, Belgium.

Despite increasing recognition of the relevance of biological cycling for Si cycling in ecosystems and for Si export from soils to fluvial systems, effects of human cultivation on the Si cycle are still relatively understudied. Here we examined stable Si isotope ($\delta^{30}Si$) signatures in soil water samples across a temperate land use gradient. We show that – independent of geological and climatological variation – there is a depletion in light isotopes in soil water of intensive croplands and managed grasslands relative to native forests. Furthermore, our data suggest a divergence in $\delta^{30}Si$ signatures along the land use change gradient, highlighting the imprint of vegetation cover, human cultivation and intensity of disturbance on $\delta^{30}Si$ patterns, on top of more conventionally acknowledged drivers (*i.e.* mineralogy and climate).

Dissolved silicate (DSi), as released from chemical weathering of silicate minerals, is involved in numerous biogeochemical reactions prior to its discharge in rivers[1,2]. Continental vegetation mediates weathering rates, in particular in soil micro-environments influenced by roots[3,4]. Yet plants can also take up considerable amounts of DSi from soil water[5,6] which can be recycled in the soil from falling litter and dissolution of the amorphous biogenic Si structures (BSi) or phytoliths in plant' tissues[2,7]. Biogenic Si production in terrestrial vegetation (84×10^{12} mol Si $year^{-1}$)[8] is at least an order of magnitude larger than the annual export of dissolved and biogenic Si towards the coastal zone[9,10] and is thus too large to be solely derived from newly mobilised Si[11]. The soil-plant system can be seen as an ecosystem filter[9] buffering the actual release of Si to rivers by recycling of reactive amorphous Si in ecosystems (soils + plants). Human activities have perturbed this terrestrial Si filter, with effects persisting in rivers, estuaries and coastal zones[9,10,12–14]. Prolonged landscape cultivation and intense agricultural expansion have lowered DSi fluxes to rivers[8,15] and diminished soil amorphous (*i.e.* both biogenic and non-biogenic) Si stocks due to agricultural Si harvest[16–18] or due to Si losses after surface erosion[12]. Although crop removal can rapidly (*i.e.* ~10 years) induce top soil depletion of phytoliths[19], timescales at which human cultivation impacts on soil Si dynamics and export from soils towards fluvial systems are not well understood[9,11]. Mechanisms controlling Si cycling in the soil-plant system are likely separated in time, from relatively quick adsorption/desorption reactions (seconds), to neoformation and dissolution of clay minerals (10–1000 years or more)[19] via the intermediate residence time of biogenic Si. Moreover, changes in clay mineralogy may be amplified by vegetation cover[20,21] and management practices in cultivated soils (*e.g.* fertiliser use)[22].

Stable Si isotopes have been successfully applied to define Si sources and sinks along the ecosystem flow path[2,21,23–27]. Intense fractionation of Si isotopes occurs during chemical weathering[27] and rivers are generally enriched in ^{30}Si isotopes ($\delta^{30}Si$ of −0.10–+4.66‰)[27,28] compared to the source bedrock[27,29] ($\delta^{30}Si$ of bulk upper continental crust is ~−0.25‰)[30]. Several mechanisms may cause this enrichment: clay neoformation[21,29,31], Si adsorption onto Fe and Al oxides[32,33] and Si uptake in plants[26,27,34]. It has been recently suggested that the light Si isotopic composition of clays formed during weathering is inherited from early fractionation during Si adsorption onto amorphous Al-hydroxides[33]. Dissolution of secondary clay minerals can therefore enrich solutions in the light isotopes. Stable Si isotopes are currently underexploited in the end-product of the soil-plant system: the soil water. Currently only a limited amount of DSi $\delta^{30}Si$ data in soil water is available and research is predominantly focused on variation within one weathering profile or within one natural ecosystem or land use type, such as forest[23] or grassland[24]. Here, we aim to isolate the role of land use change by examining the Si isotopic variation of soil water DSi in different ecosystems characteristic of Western European landscapes: i) a deciduous oak/beach forest, ii) a cultivated grassland (pasture), and iii) two croplands with row crops differing in duration of

cultivation (cropland with short (~30 years) and long (at least 240 years) duration of cultivation is called "young" and "old" cropland throughout this work). The land use change gradient is perfectly fitted to meet our objectives, as we can rely on similar bulk mineralogical and climatological properties and a considerable number (n = 102) of soil water DSi δ^{30}Si samples. Clay mineralogical differences between sites can be fully related to land-use effects. Supplementary tables S1–S6 provide further details on the land use gradient (soil characteristics, bulk and clay mineralogy,…).

Results and Discussion

A clear δ^{30}Si signature. Si isotopes were analysed on a selection of soil water DSi samples from a long-term operative sampling network (Fig. 1; Supplementary Table S7 for raw ^{30}Si, ^{29}Si and DSi data). Selection covers within-site variability, including soil depth, topographical gradients and distances along the slope perpendicular to the draining river (Supplementary Fig. S1). The highest and most stable mean soil water DSi δ^{30}Si signatures are found in the old cropland (δ^{30}Si = +1.61 ± 0.12), intermediate in pasture (δ^{30}Si = +1.05 ± 0.21) and young cropland (δ^{30}Si = +0.89 ± 0.31) while the lowest δ^{30}Si and most variable signatures derive from DSi in forest soil water (δ^{30}Si = +0.62 ± 0.34) (Fig. 1). Average soil water DSi δ^{30}Si signature differences between sites are significant ($p < 0.05$) for forest vs. pasture, forest vs. old and vs. young cropland, old vs. young cropland and pasture vs. old cropland but not for young cropland vs. pasture. Within-site variation in DSi δ^{30}Si was only significant for pasture (Supplementary Table S8–9).

Explaining δ^{30}Si variation along the land use change gradient. *Plant-soil cycle*. Soil BSi storage is strongly effected by land use changes (Fig. 2a). Biological Si recycling in the root zone has been shown to control DSi concentrations in soil and export water[7] and could partly control its δ^{30}Si, due to the discrimination against heavier isotopes of Si during plant uptake[26,27,34]. In forests, intense Si cycling occurs in the plant-soil system[2] (and references therein), with annual Si uptake into biomass equal to or larger than annual Si return to soil as litter fall, and thus a strong turnover and potentially large storage in BSi reservoirs. Given the rapid decline of BSi concentrations down the soil profile (*i.e.* from ~8 and <0.1 mg BSi/g at 5 and 40 cm respectively; Fig. 2a), long-term BSi burial in the forest soil can be omitted in this study. Light isotopes from litter are thus released into soil solution, especially during the replenishing of soil water during and after rain events[35], which occur year-round in the study area. (Semi)-natural grasslands, as well as forests, show tight Si cycling in vegetation and soil[24,36]. Some studies relate stable BSi pools of grasslands to more resistant grass phytoliths[37]. As grass species in general are the worlds' largest Si accumulators[6] and have higher BSi contents compared to forest litter (*i.e.* in this study an average of 0.9% BSi in grass versus 0.6% BSi in forest litter), they could also have a higher potential for DSi uptake and therefore a stronger impact on soil water δ^{30}Si signatures during growth. Mowing and grazing in pastures and croplands reduces the return of DSi to soil water associated with litter-decomposition, likely resulting in a generally higher DSi δ^{30}Si signature relative to forest. At the surface efficient harvest in croplands could explain the depletion of soil BSi (Fig. 2a) and higher DSi δ^{30}Si signature (Fig. 1). While the young cropland soil water DSi δ^{30}Si is still impacted by a pool of persistent soil phytoliths enriched in ^{28}Si, BSi dissolution (and associated release of ^{28}Si) is of minor importance in the old cropland. Moreover, higher DSi uptake by

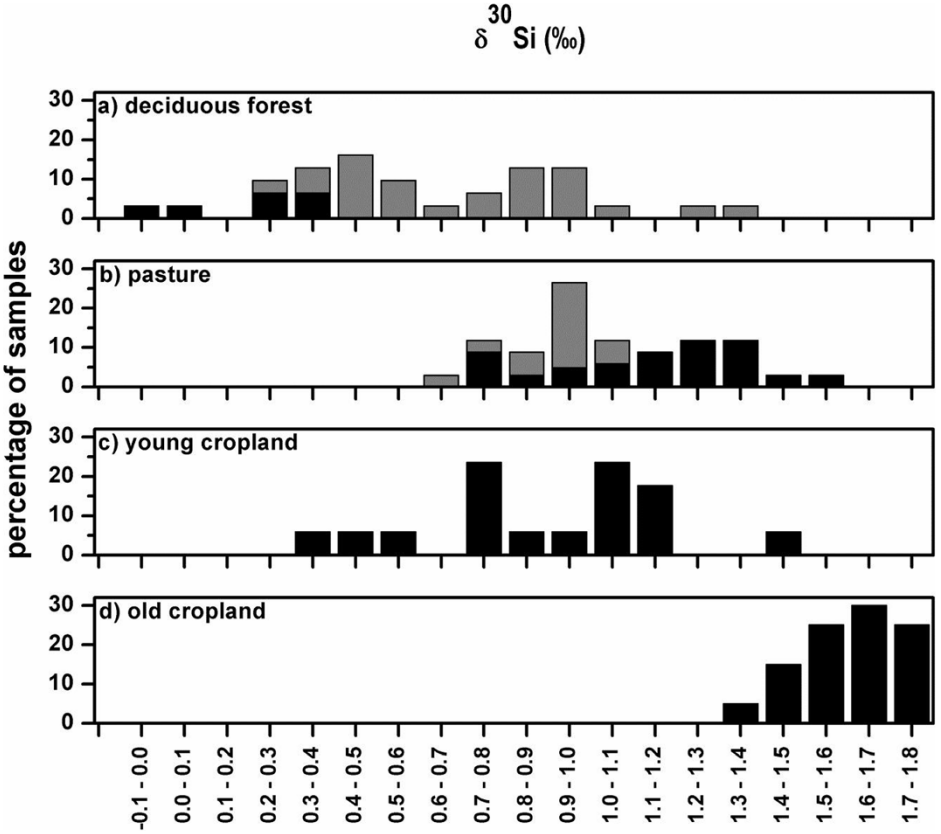

Figure 1 | Bar charts of soil water DSi δ^{30}Si in different sites. From top to bottom: (a) deciduous forest (Ronquières), (b) pasture (Blégny), (c) young cropland (Ganspoel) and (d) old cropland (Velm). Data are categorised in 19 size categories of δ^{30}Si, ranging from −0.1 to 1.8‰. The dark part of the bar shows the samples in the unsaturated soil, the grey parts of bars show the samples collected in the saturated soil. See supplementary information for more details on δ^{30}Si values and sampling selection.

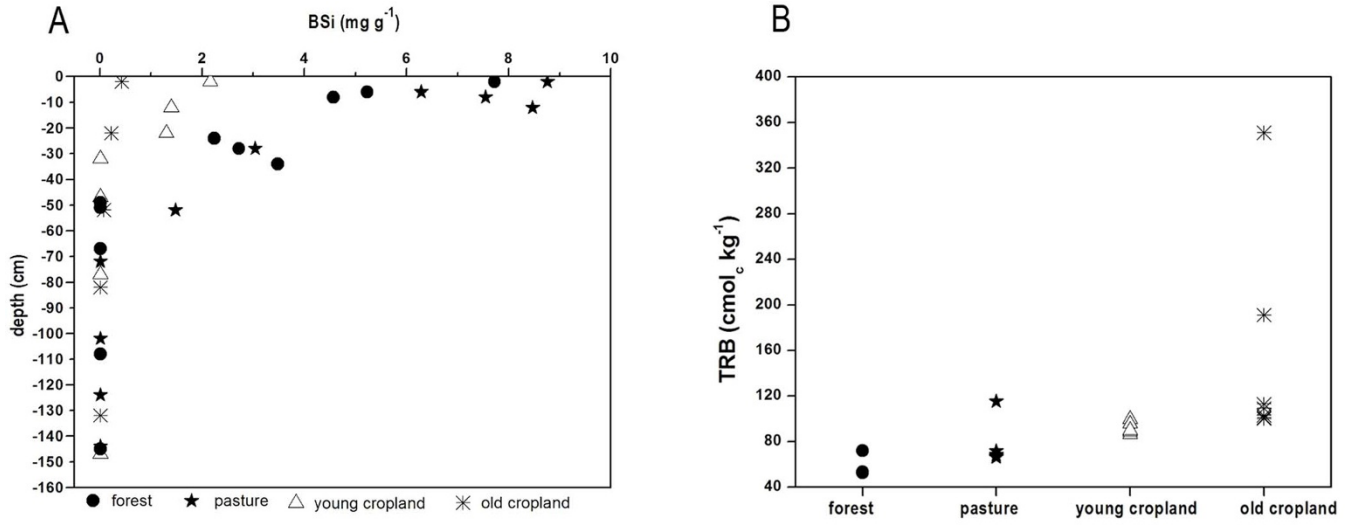

Figure 2 | (a) Scatterplot of biogenic silica (BSi) in mg g^{-1} dry soil in the soil profile, (b) Total Reserve in Bases (TRB = [Na] + [Mg] + [Ca] + [K]) weathering index calculated on dry soil, in cmol charge kg^{-1}. Sites are represented by symbols: Ronquières (circles), Blégny (stars), Ganspoel (triangle) and Velm (crosses). Multiple symbols within a site in (b) represent different TRB values calculated from positions and depths along the slope in every site for which soil water DSi δ^{30}Si are available, i.e. 3 in forests, 6 in pasture, 5 in young cropland and 7 in old cropland (See supplementary information for details).

wheat as compared to corn (in young cropland), and thus higher plant BSi content (average of 1.3% versus 0.3% BSi respectively; Supplementary Table S10) may further deplete soil in the perennial arable field, and enrich soil water with ^{30}Si.

Weathering. Despite homogeneous climate and bulk mineralogy, clay evolution and weathering regime can be altered by land use. Different Si isotope fractionations caused by clay differences could partly control soil water DSi δ^{30}Si signatures. We have indications that our forest site is more prone to chemical weathering and clay dissolution[23,38], driven by lower pH minima and higher production of organic matter. Lower values for total reserve in bases (TRB; lower TRB indicates a higher degree of soil weathering)[39] are calculated in forests than croplands (Fig. 2b). Moreover, clay diversity (especially 2 : 1) and heterogeneity along the profile is more pronounced in the forest site, which may emphasise the importance of small scale variation (as also reflected by the large range in DSi δ^{30}Si in soil water). Saturation indices in soil water show further dissolution of secondary precipitates as an important process in all land uses (Supplementary Table S11). It could be argued that higher forest heterogeneity facilitates conditions for consecutive clay dissolution and precipitation processes (*i.e.* as shown by smectite precipitation in forests in some cases). However, without clear insight into Si isotope fractionation patterns in (2 : 1) clays, impact of clay evolution on soil water DSi δ^{30}Si remains unquantified.

Other factors. Apart from Si fractionation due to plant-soil cycling of Si and weathering processes, the addition of light Si isotopes to the soil solution can be altered by other factors, such as the ratio and occurrence of adsorption/desorption processes, the use of fertiliser and impact of local hydrology. Si fractionation occurs during DSi adsorption and although quite small initially (i.e. 0.5‰) fractionations can range up to about 3‰ due to successive dissolution/precipitation and adsorption/desorption processes[27]. Low amounts of adsorbed oxalate-extractable Si are present in our soils (*i.e.* range of 0.03–0.42 mg Si_{ox}/g) and large differences in Si_{ox} between study sites are absent (Supplementary Table S5). A large impact on Si isotope fractionation driven by adsorption/desorption processes can thus probably be ruled out here. Furthermore, hydrological variations and in particular the position of the groundwater table is likely influencing soil water DSi δ^{30}Si signatures. When δ^{30}Si signatures of the unsaturated and saturated zone in pasture and forest systems are plotted separately (Fig. 1, respectively black and grey bars), differences between land use δ^{30}Si become more prominent (note: for cropland soil water δ^{30}Si there is no effect of hydrology as all soil water samples from croplands in this study are collected from the unsaturated zone). More specifically, the mean stable Si isotopic signature of soil water DSi varies within the pasture system and along the slope perpendicular to the river: highest DSi δ^{30}Si values are measured in soil water sampled from the unsaturated zone at the plateau (δ^{30}Si = +1.27 ± 0.20) and lowest values in soil water from the saturated zone in the valley (δ^{30}Si = +0.91 ± 0.11) (Supplementary Table S7 and Fig. S1). Finally, organic fertilisers (*i.e.* derived from plant remains and/or manure) applied to the croplands are unlikely to be responsible for DSi δ^{30}Si differences along the land use change gradient, as BSi input through fertilisers (*i.e.* ~10 kg of BSi ha^{-1}; Supplementary Table S10) only corresponds to circa 10% of the annual BSi export due to crop harvest (112–127 kg BSi ha^{-1} $year^{-1}$). More importantly, there is a lack of correlation between the Si isotopic composition and the fertiliser-derived elements (such as Mg and K) in the soil water of the old cropland. We therefore expect that increasing export of light ^{28}Si isotopes in cultivated land uses, and higher recycling of ^{28}Si and elevated weathering intensity (including clay dissolution) in forest systems will largely determine soil water DSi δ^{30}Si signatures of our systems (Fig. 3). Our data do not allow to distinguish biological from pedogenic processes, but point to the interaction of both. At a catchment scale, this still results in an altered Si isotope signature in most soil solutions.

Conclusions and implications. Our results imply that soil water δ^{30}Si signatures are modified through soil management before reaching rivers and coastal zones, where other fractionation processes may take over (*e.g.* diatom uptake or reverse weathering in floodplains). The imprint of land cover and its related biological and pedogenic processes is potentially high: the soil water δ^{30}Si range (−0.11–+1.81‰) in this homogeneous small scale study only impacted by a changing land use and duration of cultivation covers almost 50% of observed global riverine DSi δ^{30}Si variation (see Supplementary Fig. S2 for an overview of river, soil and groundwater DSi δ^{30}Si). As human cultivation can put constraints on the DSi δ^{30}Si soil water signal of distinct land use systems, the signal - or parts of it - can potentially be transferred to the DSi δ^{30}Si signature of adjacent fluvial systems. Indeed, our DSi δ^{30}Si soil water signal matches well with DSi δ^{30}Si variation in rivers draining

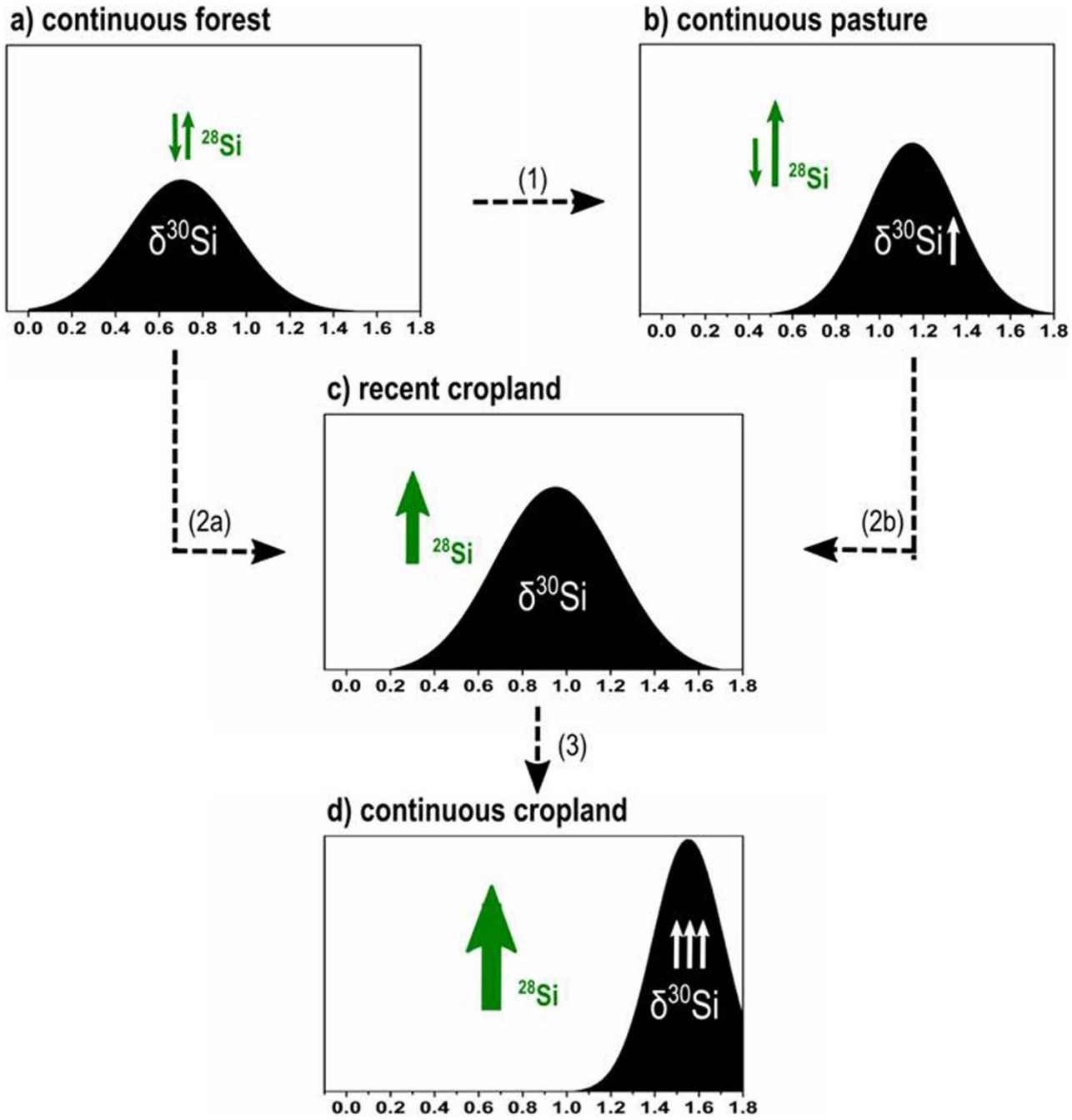

Figure 3 | Conceptual outline of land use effects on soil water DSi δ^{30}Si in a temperate weathering regime. Green arrows represent cycling and/or export of ^{28}Si, dashed arrows represent land use changes: (1) from forest (a) to pasture (b), (2a) from forest to cropland (c) and (2b) from pasture to cropland and (3) from recent (c) to continuous (d) cropland. In (a) light isotopes are intensively recycled (precipitation and dissolution), resulting in an average low δ^{30}Si signature in soil water, with a high variability. In (b) not all biomass (and light Si isotopes) is recycled, and optimal conditions for enhanced weathering and clay dissolution are absent. Soil water δ^{30}Si shifts to higher values. In c, negligible biomass returns, resulting in an increased export of ^{28}Si. In d the pool of ^{28}Si is completely exhausted and continuous harvest of ^{28}Si results in a high and consistent soil water DSi δ^{30}Si signature.

neighboring catchments in Belgium (0.46–2.09‰), which was unrelated to diatom growth, yet could be correlated to distinct vegetation covers: forest and arable land with row crops resulted in average low and high δ^{30}Si values in river water respectively[40]. Our results allow a more direct link between land cover and soil and river water DSi δ^{30}Si signatures. Future research needs to better constrain the magnitude of processes associated with Si fractionation during land cultivation. No geographical counterparts of land use change gradients currently exist, and validation of our results in other systems worldwide is essential.

A transient ^{28}Si sink? Mounting evidence challenges the steady-state of the contemporary Si cycle (*i.e.* at human time scales of less than 1000 years), as land use conversions alter or even hinder Si recycling and introduce transient non-steady state conditions of Si in terrestrial ecosystems[13,15,16,41]. Global annual agricultural Si harvest is estimated around 8 Teramole Si[42], a value which is comparable with the amount of dissolved silicate transported in rivers worldwide[10]. As at least part of the harvested Si is likely not recycled back to the soil-plant system and ends up in transient to permanent sinks (*e.g.* construction materials, sludge,…)[18,26], this

implicitly involves removal of ^{28}Si from cultivated systems. Our data strengthen the hypothesis that long-term intensive cultivation is lowering DSi export towards semi-closed coastal environments (estuaries and within restricted seas like the North Sea), yet the exact change in $\delta^{30}Si$ signal reaching rivers remains currently unquantified. Land use change effects on soil and river DSi and thus $\delta^{30}Si$ will probably become more pronounced in systems where biological cycling, uptake and fractionation of Si is very high. For example, annual uptake of dissolved Si by rice growth alone is five times higher than the Si flux in the Yangtze River[25,26] and Si sequestration in rice is at least one order of magnitude higher than concentrations of plant BSi observed in this study. Furthermore, steady state of the global biogeochemical Si cycle on longer than human timescales (>1000 years) is no longer self-evident, as lakes and reservoirs for example are likely accumulating reactive Si (including BSi) enriched with light Si isotopes[11]. Apart from having implications for estimations of weathering rates, a change in the efficiency of Si retention in lakes and reservoirs suggests that the flux and isotopic Si composition of dissolved Si reaching the ocean has varied correspondingly. As rivers supply about 85% of the annual DSi input to the surface ocean, and are the main source of Si for the ocean balancing annual export of BSi to the ocean sediments, the potential impact of a change in $\delta^{30}Si$ from continents to river on historical and contemporary productivity estimates in closed basins and coastal zones deserves better attention, as it is often assumed that the Si isotopic composition of river DSi has remained constant in time[43]. Our results demonstrate that DSi $\delta^{30}Si$ is a useful and sensitive indicator to identify and quantify impacts of human cultivation and soil disturbance on the terrestrial Si cycle, with the potential to track subtle changes in clay evolution and biogenic sink/source functions induced by land use change.

Methods

Study site description. The land use gradient is located in the loess belt of Central Belgium, where climate is temperate, without a dry season and with a warm summer (Köpper-Geiger climate map of Europe). Mean annual precipitation in all sites is estimated at ~820 mm with mean January and July temperature approximately 3°C and 18°C, respectively. The land use change gradient consists of four study sites and has been selected based on historical and current land cover. Three sites have been under perennial forest (Ronquières, dominated by >80% F. *sylvatica* and Q. *robur* sp.), pasture (Blégny) and cropland cover (Velm) for at least 240 years. One site, i.e. the recently converted cropland (Ganspoel) has only been managed as cropland since 1980 at the earliest and has had a monoculture of maize (Z. *mays L.*) for the last 14 years; before 1980 the land was used mainly as an extensive pasture with alternating periods of forest cover. The old cropland (Velm) is dominated by a rotation system with maize, wheat (T. *aestivum*) and fodder beets (B. *vulgaris*). Catchment sizes range between 34 and 230 ha (see Supplementary Table S1 for details on the land use change gradient).

Multiple soil parameters were analysed on soil cores of at least one meter (Supplementary Table S2–4; Supplementary Table S6, S9): soil bulk and clay mineralogy, pH (H_2O), particle size distribution, cation exchange capacity, biogenic Si in soils, Si adsorbed onto Fe and Al (hydr)oxides and major elemental content in soil (Al, Si, Fe, Ca, K, Na, Mg, Mn, Ti). All analyses were conducted on dried soil samples (at least 3 days at 75°C).

Soil water sampling. Soil water was collected using Teflon suction cups (Eijkelkamp) along two topographical transects in the landscape (hollow and ridge concavity), at three locations (valley, slope and plateau) and at three soil depths (30, 60 and 90 cm) (see Supplementary Fig. 1). Sampling occurred on a monthly basis at base flow conditions, during two years (2010–2011). During dry months, soil water could often not be extracted as moisture tensions in soils were higher than those imposed by the suction cup samplers. Water samples were filtered immediately after sampling through 0.20 µm soil size membranes (Chromafil Xtra MV-20/25; cellulose mixed esters) and stored at 4°C prior to analysis. A selection of soil water samples from the sampling network was used in this study, reflecting local variations (depth and distance along the gradient or to the river). Only soil water samples containing a sufficient water volume (~30 mL) could be used for stable isotope analysis. On top, hydrological conditions varied between sites. Forest and pasture catchments are drained by a small permanent stream, whereas an intermittent stream is filled by runoff in both cropland sites. Soil water in croplands is solely collected from the unsaturated zone, as groundwater tables reach a few meters deep. In the pasture catchment, the unsaturated zone is very thin (i.e. sometimes < 1 m) and suction cups placed close to the stream are continuously fed by shallow groundwater from aquifers (seeps). Soil water collected from the riparian zone within the forest was similarly mixed with deep and shallow groundwater, and only suction cups located higher on the slope collect water from the unsaturated zone (Supplementary Fig. S1).

Si isotopic analysis. Organic matrices were removed using thermal and aerobic decomposition. The solution was further purified using a cation exchange resin[44] and Si recovery and cation removal was checked after purification by ICP-MS. Si isotopic compositions were measured with a Nu Plasma Multi-Collector-ICP-MS (Nu Instrument) operating in dry plasma mode[45]. Mass bias was corrected through an external Mg doping[46]. The sample-standard bracketing technique was used to correct for the long-term instrumental drift. All results have been measured as $\delta^{30}Si$ (‰) relative to NBS28 quartz standard (National Institute of Standard and Technology, reference 8546) or an equivalent in-house standard (*Pro Analysis* Quartz from Merck) following:

$$\delta^{30}Si = \left(\left(^{30}Si/^{28}Si\right)_{sample} / \left(^{30}Si/^{28}Si\right)_{NBS28} - 1 \right) \times 1000$$

Matrix effects were corrected for by acid doping[47]. The acid doped matrix of NO_3^-, Cl^-, SO_4^{2-} and PO_4^{3-} was adjusted to 500 mg L^{-1}, 100 mg L^{-1}, 200 mg L^{-1} and 50 mg L^{-1}, respectively. All samples were replicated in different analytical sessions distributed over several months and all samples were fully replicated at least once. The accuracy of the DSi $\delta^{30}Si$ measurements was checked on a daily basis by measuring a secondary reference material of known isotopic composition (diatomite)[48]. Long-term average analytical reproducibility on sample full duplicates and accuracy on this reference material for $\delta^{30}Si$ was ±0.14‰ ($\pm 2\sigma_{SD}$). On a $\delta^{29}Si$–$\delta^{30}Si$ plot[49] (Supplementary Fig. S3) all samples define ($R^2 = 0.985$) a mass-dependent fractionation line $\delta^{29}Si = \delta^{30}Si^{\beta}$ with $\beta = 0.5108$, closer to kinetic fractionation ($\beta = 0.5092$) than to an equilibrium fractionation ($\beta = 0.5178$). On the same samples used for Si isotopic analysis, DSi concentrations (molybdenum-blue colorimetric method) and concentration of major cations (K^+, Na^+, Mg^{2+}, Ca^{2+}, Al^{3+}, Mn^{2+}; ICP-MS) were measured (Supplementary Table S12).

Statistics. Statistical tests were performed using IBM SPSS package. One – way ANOVA and Scheffe test for multiple comparisons were conducted to test mean differences in DSo $\delta^{30}Si$ between sites, depths within sites, seasonal variation within sites and distance to river within sites. If the assumption of normality (Shapiro-Wilk statistic) was not supported, or group variances were not homogeneous (Levene test statistic), alternative statistics to test mean differences and multiple comparisons were used (*i.e.* Welch ANOVA and Games-Howell test). Details on the statistical tests can be found in Supplementary Table S8 and S9.

1. Sommer, M., Kaczorek, D., Kuzyakov, Y. & Breuer, J. Silicon pools and fluxes in soils and landscapes - a review. *J. Plant Nutr. Soil Sc.* **169**, 310–329 (2006).
2. Cornelis, J. T. *et al*. Tracing the origin of dissolved silicon transferred from various soil-plant systems towards rivers: a review. *Biogeosciences* **8**, 89–112 (2011).
3. Calvaruso, C., Mareschal, L. & Turpault, M. P. Rapid clay weathering in the rhizosphere of Norway Spruce and oak in an acid forest ecosystem. *Soil Sci. Soc. Am. J.* **73**, 331–338 (2009).
4. Hinsinger, P., Fernandes Barros, O. N., Benedetti, M. F., Noack, Y. & Callot, G. Plant-induced weathering of a basaltic rock: experimental evidence. *Geochim. Cosmochim. Ac.* **65**, 137–152 (2001).
5. Epstein, E. Silicon. *Annu. Rev. Plant Phys.* **50**, 641–664 (1999).
6. Hodson, M. J., White, P. J., Mead, A. & Broadley, M. R. Phylogenetic variation in the silicon composition of plants. *Ann. Bot.* **96**, 1027–1046 (2005).
7. Derry, L. A., Kurtz, A. C., Ziegler, K. & Chadwick, O. A. Biological control of terrestrial silica cycling and export fluxes to watersheds. *Nature* **433**, 728–731 (2005).
8. Carey, J. C. & Fulweiler, R. W. The terrestrial silica pump. *Plos One* **7**, e52932 (2012).
9. Struyf, E. & Conley, D. Emerging understanding of the ecosystem silica filter. *Biogeochemistry* **107**, 9–18 (2012).
10. Treguer, P. J. & De La Rocha, C. L. The world ocean silica cycle. *Ann. Rev. Mar. Sci.* **5**, 477–501 (2013).
11. Frings, P. *et al*. Lack of steady-state in the global biogeochemical Si cycle: emerging evidence from lake Si sequestration. *Biogeochemistry* **117**, 255–277 (2014).
12. Conley, D. J. *et al*. Deforestation causes increased dissolved silicate losses in the Hubbard Brook Experimental Forest. *Global Change Biol.* **14**, 2548–2554 (2008).
13. Struyf, E. *et al*. Historical land use change has lowered terrestrial silica mobilization. *Nature Communications* **1**, 129 (2010).
14. Laruelle, G. G. *et al*. Anthropogenic perturbations of the silicon cycle at the global scale: Key role of the land-ocean transition. *Global Biogeochem. Cy.* **23**, GB4031 (2009).
15. Carey, J. C. & Fulweiler, R. W. Human activities directly alter watershed dissolved silica fluxes. *Biogeochemistry* **111**, 125–138 (2012).
16. Clymans, W., Struyf, E., Govers, G., Vandevenne, F. & Conley, D. J. Anthropogenic impact on amorphous silica pools in temperate soils. *Biogeosciences* **8**, 2281–2293 (2011).
17. Guntzer, F., Keller, C., Poulton, P. R., McGrath, S. P. & Meunier, J.-D. Long-term removal of wheat straw decreases soil amorphous silica at Broadbalk, Rothamsted. *Plant Soil* **352**, 173–184 (2012).

18. Vandevenne, F., Struyf, E., Clymans, W. & Meire, P. Agricultural silica harvest: have humans created a new loop in the global silica cycle? *Fron. Ecol. Environ.* **10**, 243–248 (2012).
19. Keller, C., Guntzer, F., Barboni, D., Labreuche, J. & Meunier, J. D. Impact of agriculture on the Si biogeochemical cycle: Input from phytolith studies. *C. R. Geosci.* **344**, 739–746 (2012).
20. Collignon, C., Ranger, J. & Turpault, M. P. Seasonal dynamics of Al- and Fe-bearing secondary minerals in an acid forest soil: influence of Norway spruce roots (Picea abies (L.) Karst.). *Eur. J. Soil Sci.* **63**, 592–602 (2012).
21. Cornelis, J. T. *et al.* Silicon isotopes record dissolution and re-precipitation of pedogenic clay minerals in a podzolic chronosequence. *Geoderma* **235–236**, 19–29 (2014).
22. Cornu, S., Montagne, D., Hubert, F., Barre, P. & Caner, L. Evidence of short-term clay evolution in soils under human impact. *C. R. Geosci.* **344**, 747–757 (2012).
23. Cornelis, J. T. *et al.* Tracing mechanisms controlling the release of dissolved silicon in forest soil solutions using Si isotopes and Ge/Si ratios. *Geochim. Cosmochim. Ac.* **74**, 3913–3924 (2010).
24. White, A. F. *et al.* Biogenic and pedogenic controls on Si distributions and cycling in grasslands of the Santa Cruz soil chronosequence, California. *Geochim. Cosmochim. Ac.* **94**, 72–94 (2012).
25. Ding, T., Wan, D., Wang, C. & Zhang, F. Silicon isotope compositions of dissolved silicon and suspended matter in the Yangtze River, China. *Geochim. Cosmochim. Ac.* **68**, 205–216 (2004).
26. Ding, T. P. *et al.* Silicon isotope fractionation between rice plants and nutrient solution and its significance to the study of the silicon cycle. *Geochim. Cosmochim. Ac.* **72**, 5600–5615 (2008).
27. Opfergelt, S. & Delmelle, P. Silicon isotopes and continental weathering processes: Assessing controls on Si transfer to the ocean. *C. R. Geosci.* **344**, 723–738 (2012).
28. Cockerton, H. E. *et al.* Stable-isotope (H, O, and Si) evidence for seasonal variations in hydrology and Si cycling from modern waters in the Nile Basin: implications for interpreting the Quaternary record. *Quat. Sci. Rev.* **66**, 4–21 (2013).
29. Ziegler, K., Chadwick, O. A., Brzezinski, M. A. & Kelly, E. F. Natural variations of δ30Si ratios during progressive basalt weathering, Hawaiian Islands. *Geochim. Cosmochim. Ac.* **69**, 4597–4610 (2005).
30. Savage, P. S., Georg, R. B., Williams, H. M. & Halliday, A. N. The silicon isotope composition of the upper continental crust. *Geochim. Cosmochim. Ac.* **109**, 384–399 (2013).
31. Ziegler, K., Chadwick, O. A., White, A. F. & Brzezinski, M. A. δ^{30}Si systematics in a granitic saprolite, Puerto Rico. *Geology* **13**, 817–820 (2005).
32. Delstanche, S. *et al.* Silicon isotopic fractionation during adsorption of aqueous monosilicic acid onto iron oxide. *Geochim. Cosmochim. Ac.* **73**, 923–934 (2009).
33. Oelze, M., von Blanckenburg, F., Hoellen, D., Dietzel, M. & Bouchez, J. Si stable isotope fractionation during adsorption and the competition between kinetic and equilibrium isotope fractionation: Implications for weathering systems. *Chem. Geol.* **380**, 161–171 (2014).
34. Ding, T. P. *et al.* Silicon isotope fractionation in bamboo and its significance to the biogeochemical cycle of silicon. *Geochim. Cosmochim. Ac.* **72**, 1381–1395 (2009).
35. Clymans, W. *et al.* Temporal dynamics of bio-available Si fluxes in a temperate forested catchment (Meerdaal forest, Belgium). *Biogeochemistry* **116**, 275–291 (2013).
36. Blecker, S. W., McCulley, R. L., Chadwick, O. A. & Kelly, E. F. Biologic cycling of silica across a grassland bioclimosequence. *Global Biogeochem. Cy.* **20**, GB3023 (2006).
37. Bartoli, F. & Wilding, L. P. Dissolution of Biogenic Opal as a Function of its Physical and Chemical Properties. *Soil Sci. Soc. Am. J.* **44**, 873–878 (1980).
38. Oliva, P. *et al.* The effect of organic matter on chemical weathering: Study of a small tropical watershed: Nsimi-Zoetele site, Cameroon. *Geochim. Cosmochim. Ac.* **63**, 4013–4035 (1999).
39. Herbillon, A. J. [Chemical estimation of weatherable minerals present in diagnostic horizons of low activity clay soils] *Proceedings of the 8th International Clay Classification Workshop: Classification, Characterization and Utilization of Oxisols (part 1)* [Beinroth, F. H., Camargo, M. N. and Eswaran (ed.)] [39–48] (Rio de Janeiro, 1986).
40. Delvaux, C. *et al.* Controls on riverine δ^{30}Si signatures in a temperate watershed under high anthropogenic pressure (Scheldt - Belgium). *J. Marine Syst.* **128**, 40–51 (2013).
41. Sommer, M. *et al.* Si cycling in a forest biogeosystem - the importance of transient state biogenic Si pools. *Biogeosciences* **10**, 4991–5007 (2013).
42. Matichenkov, V. V. & Bocharnikova, E. A. [The relationship between silica and soil physical and chemical properties] *Silica in Agriculture* [Datnoff, L. E., Snyder, G. & Korndörfer, G. (ed.)] (Elsevier, Amsterdam, Netherlands, 2001).
43. Opfergelt, S., Burton, K. W., Pogge von Strandmann, P. A. E., Gislason, S. R. & Halliday, A. N. Riverine silicon isotope variations in glaciated basaltic terrains: Implications for the Si delivery to the ocean over glacial–interglacial intervals. *Earth Planet. Sc. Lett.* **369–370**, 211–219 (2013).
44. Georg, R. B., Reynolds, B. C., Frank, M. & Halliday, A. N. New sample preparation techniques for the determination of Si isotopic compositions using MC-ICPMS. *Chem. Geol.* **235**, 95–104 (2006).
45. Abraham, K. *et al.* delta Si-30 and delta Si-29 determinations on USGS BHVO-1 and BHVO-2 reference materials with a new configuration on a nu plasma multi-collector ICP-MS. *Geostand. Geoanal. Res.* **32**, 193–202 (2008).
46. Cardinal, D., Alleman, L. Y., de Jong, J., Ziegler, K. & Andre, L. Isotopic composition of silicon measured by multicollector plasma source mass spectrometry in dry plasma mode. *J. Anal. Atom. Spectrom.* **18**, 213–218 (2003).
47. Huyges, H. *et al.* Effect of seasonal biogenic silica variations on dissolved silicon fluxes and isotopic signatures in the Congo River. *Limnol. Oceanogr.* **56**, 551–561 (2011).
48. Reynolds, B. C. *et al.* An inter-laboratory comparison of Si isotope reference materials. *J. Anal. Atom. Spectrom.* **22**, 561–568 (2007).
49. Georg, R. B., Reynolds, B. C., West, A. J., Burton, K. W. & Halliday, A. N. Silicon isotope variations accompanying basalt weathering in Iceland. *Earth Planet. Sc. Lett.* **261**, 476–490 (2007).

Acknowledgments

F.I.V. thanks Special Research Funding of the University of Antwerp (BOF-UA) for PhD fellowship funding and Patrick Frings and Ryan Taylor for editing the manuscript as native speakers. We also acknowledge Flemish Science Foundation (FWO) for funding the project "Tracking the biological control on Si mobilisation in upland ecosystems" (project number G014609N) and BELSPO for funding the project SOGLO.

Author contributions

F.I.V. collected the samples and wrote the first drafts. C.D. and H.H. optimised and developed the isotopic analytical method, analysed the samples, made the data processing, and C.D., H.H. and J-T C. co-developed the discussion. F.I.V., W.C., E.S., G.G. and B.R. were involved in site selection and/or installation of the land use gradient. B.R. and A.L.B. provided background data on clay analysis and Si fractions in the soil. P.M., E.S., L.A. and G.G. initialised and conceptualised the work on Si biogeochemistry in joint collaborations. All authors contributed to the writing and methodological development of the paper.

Additional information

Supplementary information accompanies this paper at http://www.nature.com/scientificreports

Competing financial interests: The authors declare no competing financial interests.

How to cite this article: Vandevenne, F.I. *et al.* Landscape cultivation alters δ^{30}Si signature in terrestrial ecosystems. *Sci. Rep.* **5**, 7732; DOI:10.1038/srep07732 (2015).

SCIENTIFIC REPORTS

DOI: 10.1038/srep08609

SUBJECT AREAS:
BIOGEOCHEMISTRY
GEOCHEMISTRY

SCIENTIFIC REPORTS:
5 : 7732
DOI: 10.1038/srep07732
(2015)

Published:
13 January 2015

Updated:
17 March 2015

CORRIGENDUM: Landscape cultivation alters $\delta^{30}Si$ signature in terrestrial ecosystems

Floor I. Vandevenne[1], Claire Delvaux[2], Harold J. Hughes[2], Luc André[2], Benedicta Ronchi[3], Wim Clymans[4], Lúcia Barão[1], Jean-Thomas Cornelis[5,6], Gerard Govers[3], Patrick Meire[1] & Eric Struyf[1]

[1]Department of Biology, Research Group Ecosystem Management, University of Antwerp, Wilrijk, Belgium, [2]Department of Geology and Mineralogy, Royal Museum for Central Africa, Tervuren, Belgium, [3]Department of Earth and Environmental Sciences, Catholic University of Leuven, Heverlee, Belgium, [4]Department of Geology, Lund University, Lund, Sweden, [5]Department BIOSystem Engineering, University of Liège, Gembloux, Belgium, [6]Earth and Life Institute, Université catholique de Louvain, Louvain-la-Neuve, Belgium.

Jean-Thomas Cornelis was included in the Acknowledgements but omitted from the author list in the original version of this Article. This has been corrected in the PDF and HTML versions of the Article and in the Supplementary Information.

Acknowledgements

"F.I.V. thanks Special Research Funding of the University of Antwerp (BOF-UA) for PhD fellowship funding and Patrick Frings, Ryan Taylor and Jean-Thomas Cornelis for proof-reading and editing the manuscript. We also acknowledge Flemish Science Foundation (FWO) for funding the project "Tracking the biological control on Si mobilisation in upland ecosystems" (project number G014609N)."

Now reads

"F.I.V. thanks Special Research Funding of the University of Antwerp (BOF-UA) for PhD fellowship funding and Patrick Frings and Ryan Taylor for editing the manuscript as native speakers. We also acknowledge Flemish Science Foundation (FWO) for funding the project "Tracking the biological control on Si mobilisation in upland ecosystems" (project number G014609N) and BELSPO for funding the project SOGLO."

Author contributions

"F.I.V. collected the samples and wrote the first drafts. C.D. and H.H. optimised and developed the isotopic analytical method, analysed the samples, made the data processing, and co-developed the discussion. F.I.V., W.C., E.S., G.G. and B.R. were involved in site selection and/or installation of the land use gradient. B.R. and A.L.B. provided background data on clay analysis and Si fractions in the soil. P.M., E.S., L.A. and G.G. initialised and conceptualised the work on Si biogeochemistry in joint collaborations. All authors contributed to the writing and methodological development of the paper."

Now reads

"F.I.V. collected the samples and wrote the first drafts. C.D. and H.H. optimised and developed the isotopic analytical method, analysed the samples, made the data processing, and C.D., H.H. and J-T C. co-developed the discussion. F.I.V., W.C., E.S., G.G. and B.R. were involved in site selection and/or installation of the land use gradient. B.R. and A.L.B. provided background data on clay analysis and Si fractions in the soil. P.M., E.S., L.A. and G.G. initialised and conceptualised the work on Si biogeochemistry in joint collaborations. All authors contributed to the writing and methodological development of the paper."

The original Article contained an error in the calculation of the weathering index Total Reserve in Bases (TRB) in figure 2b. The correct figure 2 appears below as Figure 1.

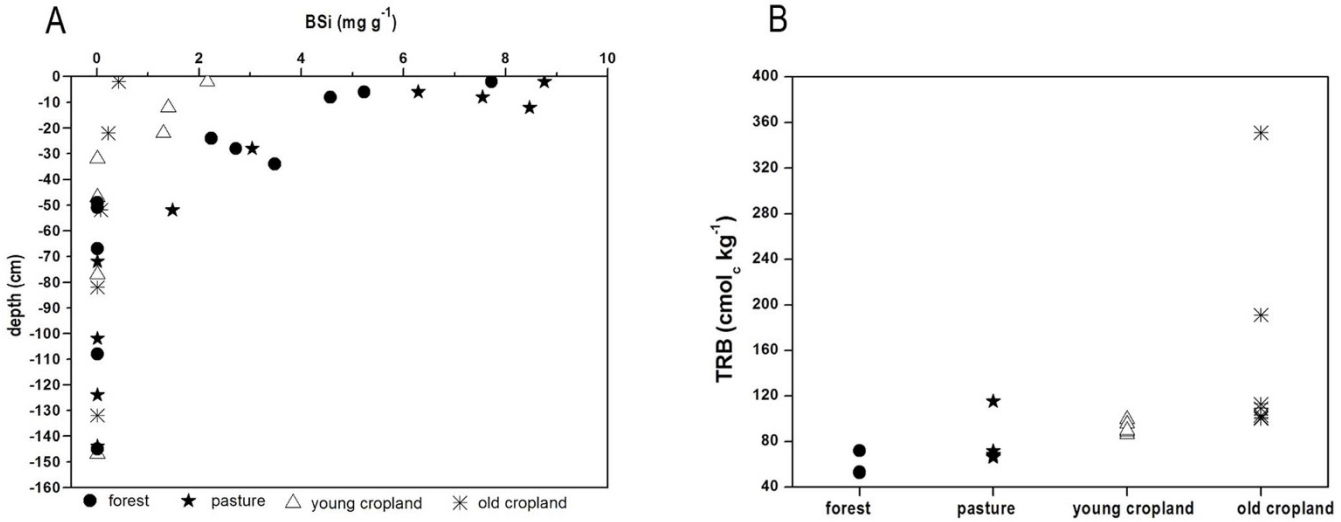

Figure 1 | (a) Scatterplot of biogenic silica (BSi) in mg g^{-1} dry soil in the soil profile, (b) Total Reserve in Bases (TRB = [Na] + [Mg] + [Ca] + [K]) weathering index calculated on dry soil, in cmol charge kg^{-1}. Sites are represented by symbols: Ronquières (circles), Blégny (stars), Ganspoel (triangle) and Velm (crosses). Multiple symbols within a site in (b) represent different TRB values calculated from positions and depths along the slope in every site for which soil water DSi $\delta^{30}Si$ are available, i.e. 3 in forests, 6 in pasture, 5 in young cropland and 7 in old cropland (See supplementary information for details).